3/8/95

SAND94-0785•UC—235
Unlimited Release
Printed February 1995

Optical Performance of the TBC-2 Solar Collector Before and After the 1993 Mirror Lustering

Richard M. Houser and John W. Strachan

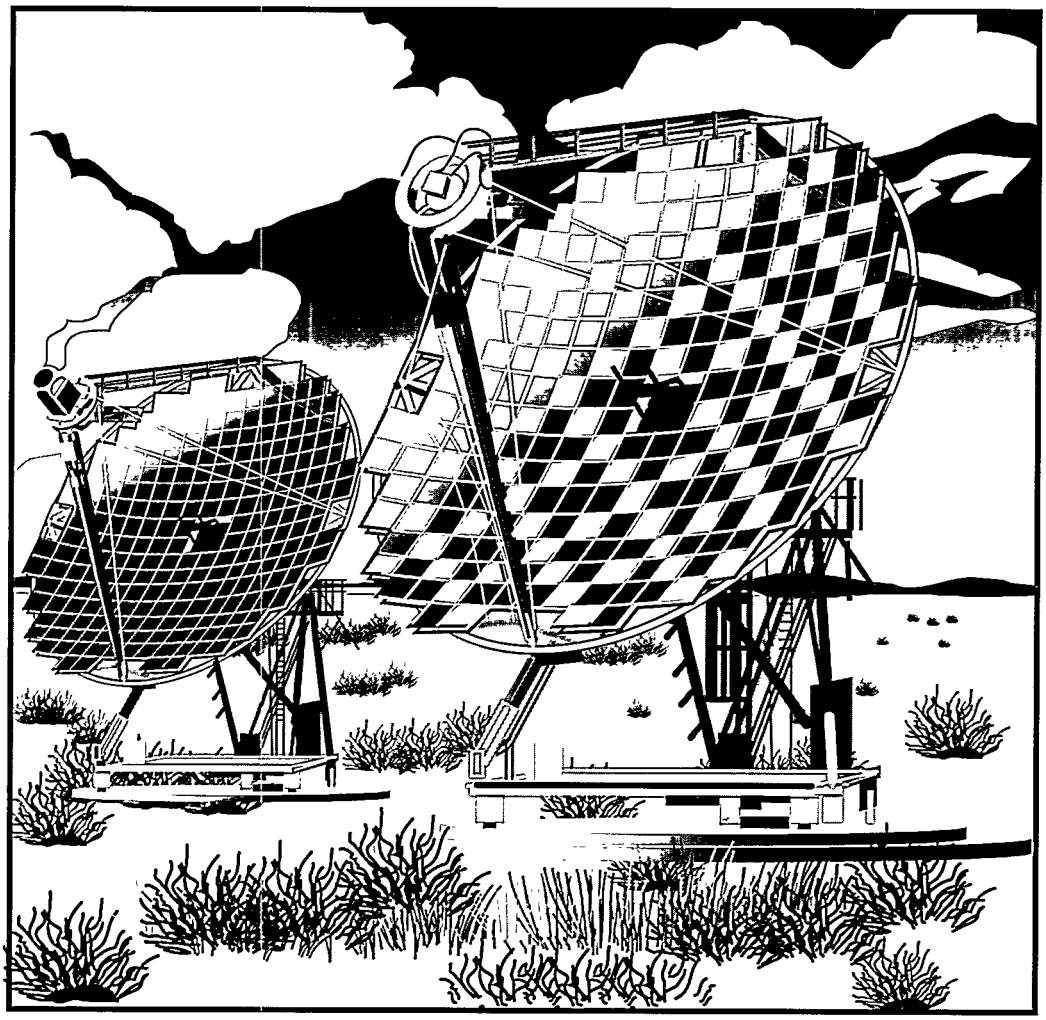

Prepared by
Sandia National Laboratories
Albuquerque, New Mexico 87185 and Livermore, California 94550
for the United States Department of Energy
under Contract DE-AC04-94AL85000

Issued by Sandia National Laboratories, operated for the United States Department of Energy by Sandia Corporation.

Available to DOE and DOE contractors from
Office of Scientific and Technical Information
PO Box 62
Oak Ridge, TN 37831

Prices available from (615) 576-8401, FTS 626-8401

Available to the public from
National Technical Information Service
US Department of Commerce
5285 Port Royal Rd
Springfield, VA 22161

NTIS price codes
Printed copy: A03
Microfiche copy: A01

SAND94-0785
Unlimited Release
Printed February 1995

Distribution
Category UC-235

OPTICAL PERFORMANCE OF THE TBC-2 SOLAR COLLECTOR BEFORE AND AFTER THE 1993 MIRROR LUSTERING

Richard Houser and John Strachan
Solar Thermal Test Department
Sandia National Laboratories
Albuquerque, NM 87185-6215

Abstract

In 1993, the mirror facets of one of Sandia's point-focusing solar collectors, the Test Bed Concentrator #2 (TBC-2), were reconditioned. The concentrator's optical performance was evaluated before and after this operation. This report summarizes and compares the results of these tests. The tests demonstrated that the concentrator's total power and peak flux were increased while the overall flux distribution in the focal plane remained qualitatively the same.

LW

Contents

Figures

Tables

INTRODUCTION

In the summer and fall of 1993, the mirrored surfaces of Sandia National Laboratories' (Sandia's) Test Bed Concentrator #2 (TBC-2) were reconditioned, or lustered. This report presents the results of the dish's optical performance before and after this lustering process. The tests described in this report were performed using Sandia's Beam Characterization System (BCS) [1,2], as well as cold water calorimetry (CWC). The BCS facilitates the measurement of the flux in the dish's focal region; it includes a diffusively reflective flux target that is positioned in the focal region, and a digital camera that is used to capture an image of the flux reflected from the target. Two flux gauges embedded in the flux target provide absolute measures of the flux density at two points on the target. The peak flux and the overall power in the beam can be obtained from the BCS as well as a flux map. For dish-type collectors the accuracy (standard deviation of expected error) of the BCS is 6 to 10%.

The BCS flux target employed in the evaluation of the TBC-2 is a circular 30-inch (in.)-diameter water-cooled aluminum plate with a Lambertian aluminum-oxide surface. It was mounted to the receiver ring of the TBC-2 (the ring is indicated by the arrow in Figure 1), and positioned along the axis of the dish by a linear actuator.

The performance testing of the "prelustered" dish took place on January 20 and 21, 1993, and the postluster tests were performed on December 22, 1993, and January 3, 1994. The two-part objective of both the before and after optical evaluations was a) to determine the location of the dish's focal plane and b) to characterize the flux at the focus and in the region behind it, in the region of the receiver.

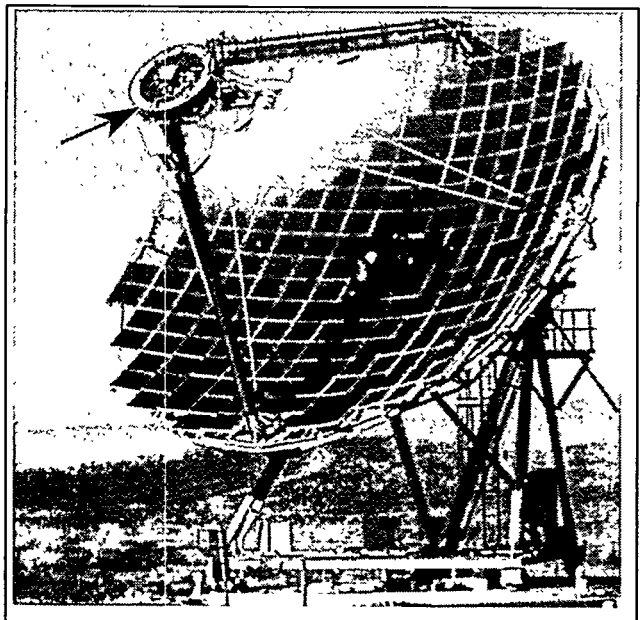

Figure 1. TBC-2 test configuration showing flux target location

FOCAL PLANE DETERMINATION TEST

For the purpose of this text a flux target is moved through the focal point while images and sensor data are acquired. These data are then reduced using a spreadsheet program to obtain the relative peak flux, relative power, and the diameter of a circle containing all flux equal to or greater than 10% of the value of the peak flux. Other than setting up the zoom, f-stop, and focus near the focal point, no corrections were made for scaling changes attributable to the change in the camera-to-target distance as the target is moved. While it is true that this introduces errors into the resulting fluxmaps, it does not prevent researchers from getting a sufficiently accurate relative measure of beam power and beam diameter at the selected positions in the focal region.

The before-and-after focal plane location test indicates that the dish's focal plane did not change significantly and is located 71.8 cm (28.3 in.) toward the vertex from the dish reference plane (see Table 1 and Figure 2).

Table 1. Beam Measurements in Focal Region During Focal Plane Determination Test

Before Lustering Day 20 (1993) at 11:45 AM Insolation: 0.895 kW/m²				After Lustering Day 356 (1993) at 11:45 AM Insolation: 0.996 kW/m²			
Position Relative to Ref. Point (cm)	Relative Power (% of Max.)	Relative Peak Flux (% of Max.)	Beam Diameter (cm)	Position Relative to Ref. Point (cm)	Relative Power (% of Max.)	Relative Peak Flux (% of Max.)	Beam Diameter (cm)
69.1	97.8	89.1	98.4	69.2	97.4	90.8	99.1
69.7	98.5	94.1	94.3	69.8	97.5	94.3	96.4
70.4	98.9	97.5	91.1	70.4	97.8	96.9	93.7
71.1	99.4	99.2	88.6	71.0	99.3	98.7	91.9
71.6	99.4	100.0	87.8	71.5	99.4	100.0	91.9
72.4	99.7	99.2	87.8	72.2	99.6	99.6	91.9
73.1	100.0	97.5	90.2	72.7	99.0	97.8	93.7
73.6	99.9	94.1	93.5	73.0	99.3	96.5	94.6
74.4	99.8	88.7	97.6	73.6	99.1	93.9	97.3
75.0	99.3	84.5	100.0	73.9	98.7	91.7	99.1
74.8	99.7	84.9	100.0	74.2	98.6	90.0	100.0

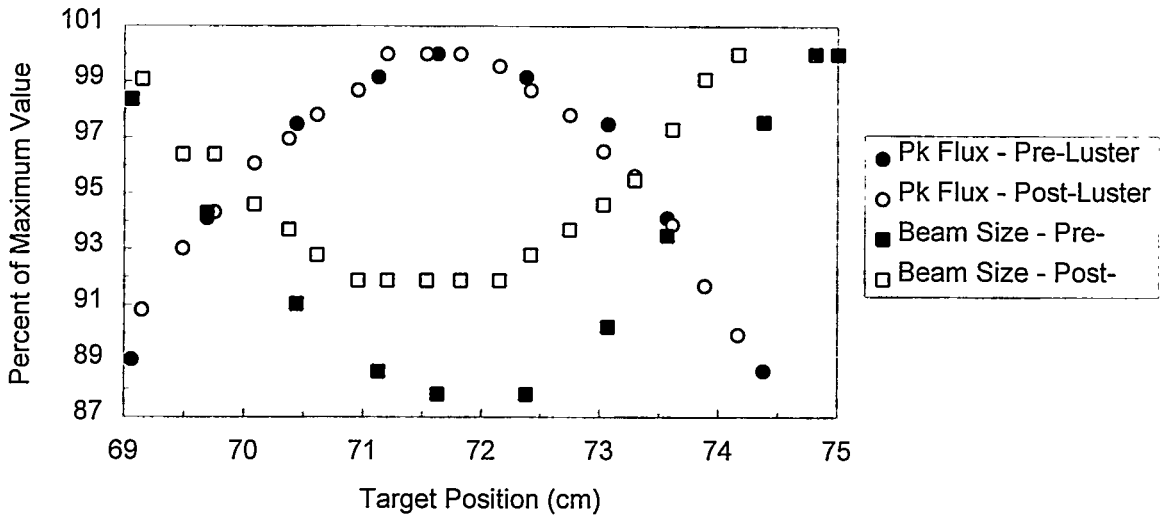

Figure 2. Location of dish's focal plane before and after lustering process

RECEIVER PLANE FLUX DISTRIBUTION TEST

Flux Distribution

Before and after the TBC-2 lustering, the dish's flux distribution at the focal plane and in the region behind it was characterized using the BCS. Flux maps were obtained at the focal plane[1] and at four positions behind it: 8.1 cm (3.2 in.), 15.7 cm (6.2 in.), 23.3 cm (9.2 in.), and 30.9 cm (12.2 in.). Color contour plots of the flux distribution at these five locations are presented in Figures 3 through 7.

A BCS image was acquired of the flux on the target while positioned at each focal plane location. Sensor data from the flux gauges were acquired simultaneously as was an insolation reading from a normal incidence pyroheliometer, or NIP. The target flux measurements were equated to the corresponding image intensity levels in the BCS image to obtain a measure of the peak flux. The image picture levels (pixel levels) were integrated using this peak flux value to estimate the total beam power. The effective beam diameter was obtained using the BCS's image analysis software functions. The TBC-2's peak flux, power, and beam diameter at the selected positions before and after the lustering process are presented in this report.

The flux maps indicate that qualitatively the distribution of flux in the focal region did not change as a result of the lustering process (see Figures 3 through 7). However, the peak flux that the dish is capable of producing did increase. Prior to the lustering of the TBC-2 mirrors, the

[1] The focal point is located 71.8 cm [28.3 in.] toward the vertex from the reference plane.

peak flux at the focal plane was 16,598 kW/m^2 (Table 2); after lustering and realignment the peak flux measured 17,953 kW/m^2, an increase of approximately 7.5%. Figure 8 shows the peak flux values before and after the lustering process as measured with the BCS and normalized to the average total power measured by CWC (pre-luster calorimetry was performed in May and June 1993 and post-luster calorimetry in November 1993). There is an unexpected drop in the 63.8-cm (25.1-in.) target position following the lustering and realignment. This lower flux level was observed on both postluster test dates (December 22, 1993 and January 3, 1994) and is unexplained at the present.

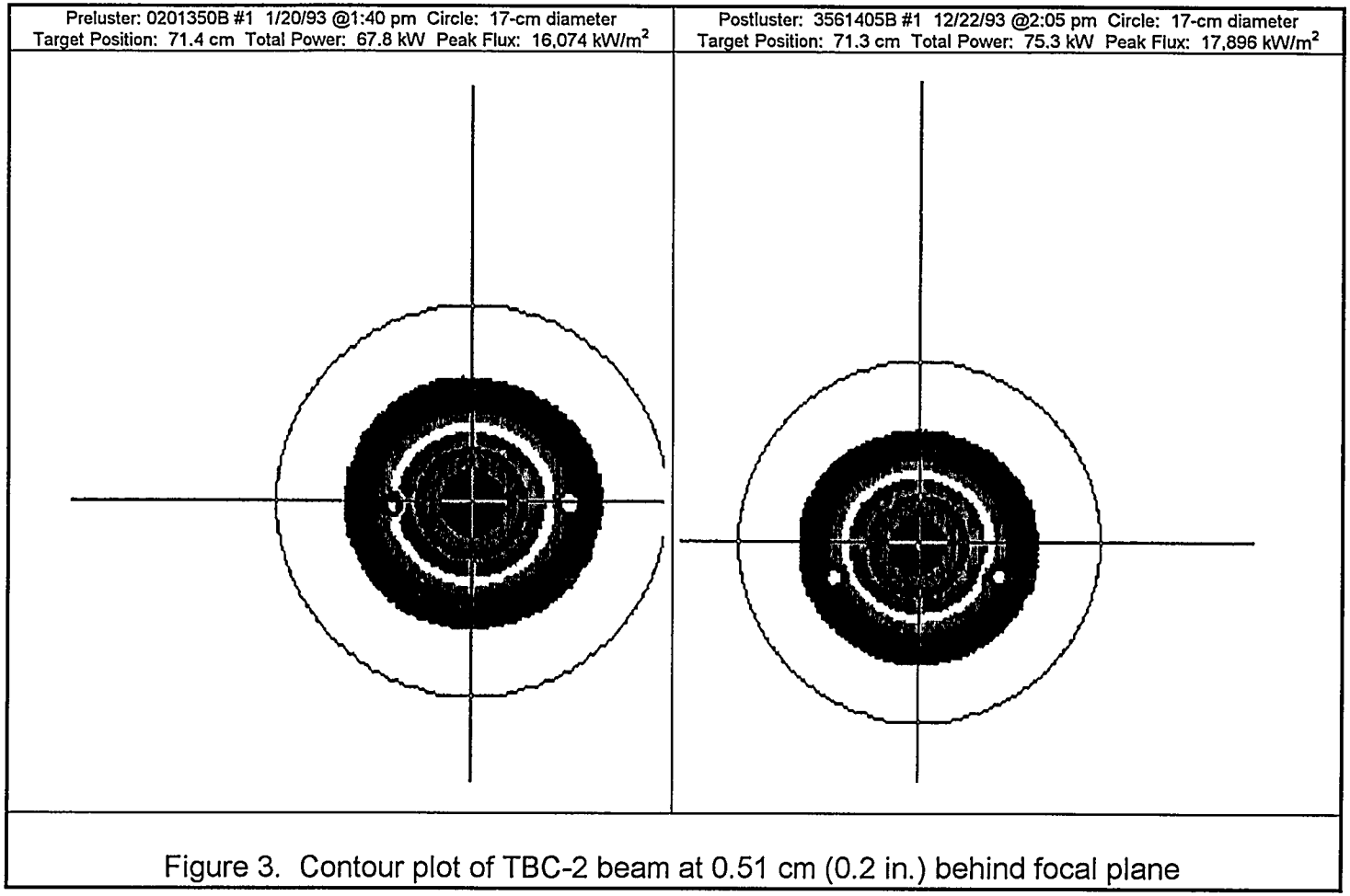

Figure 3. Contour plot of TBC-2 beam at 0.51 cm (0.2 in.) behind focal plane

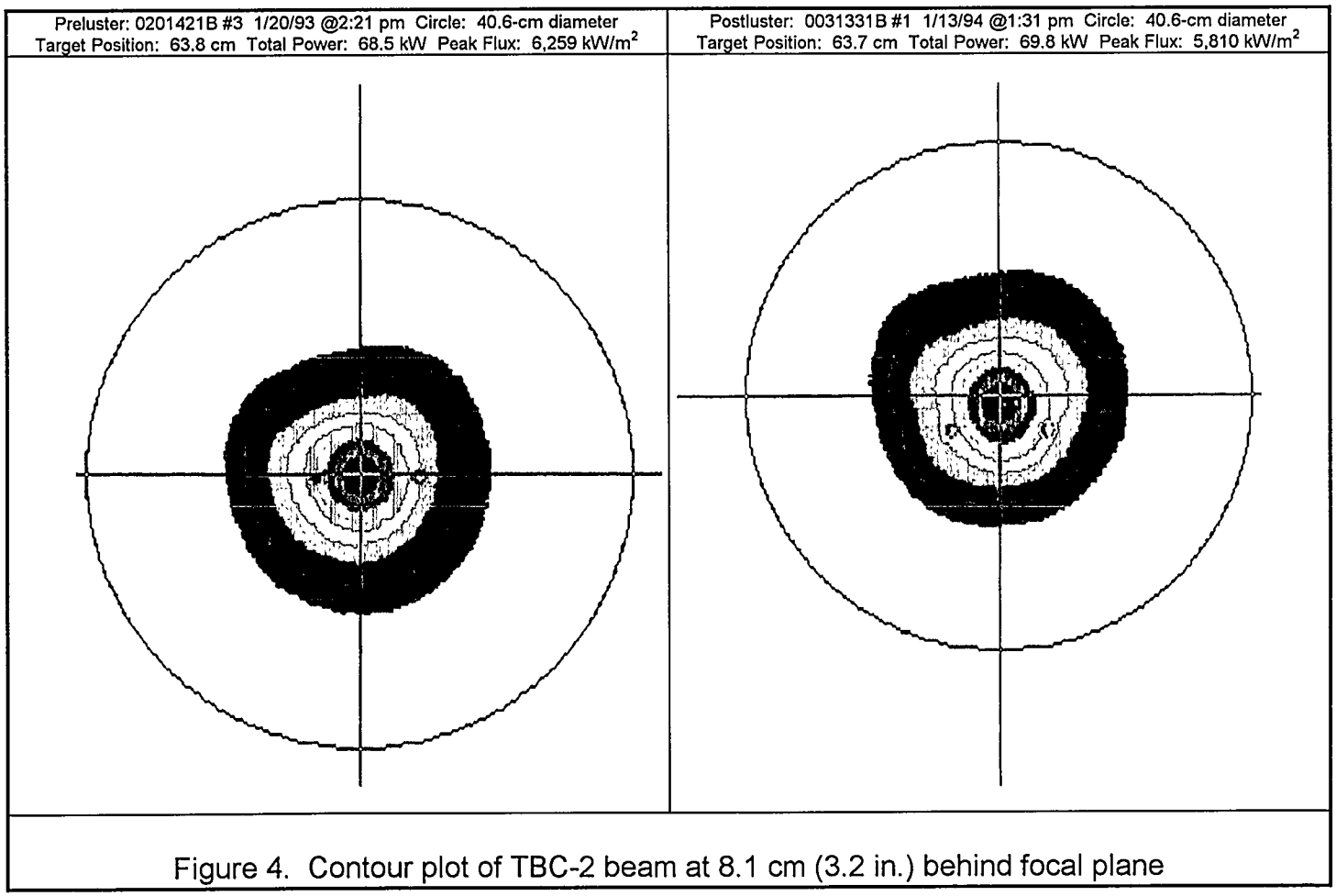

Figure 4. Contour plot of TBC-2 beam at 8.1 cm (3.2 in.) behind focal plane

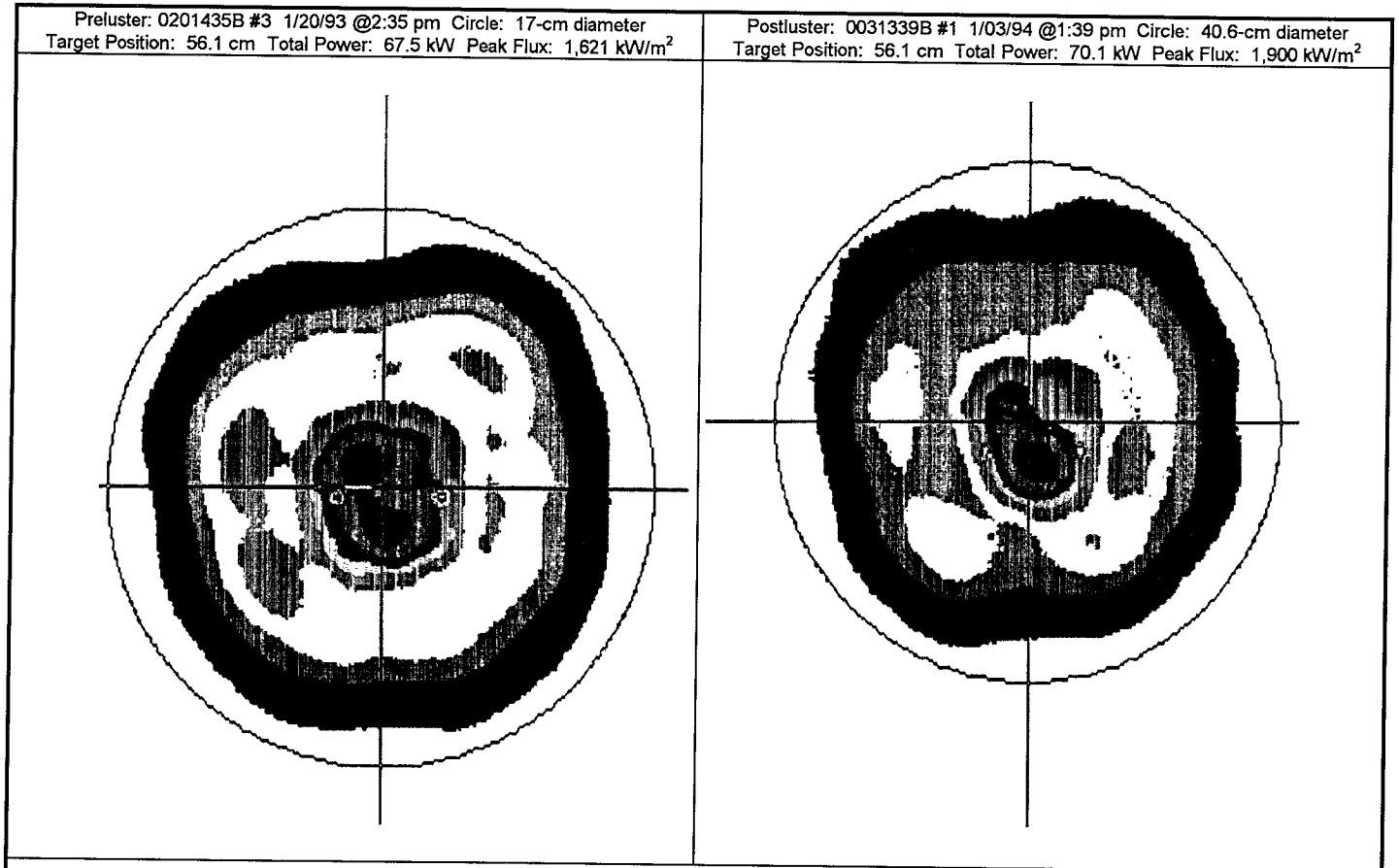

Figure 5. Contour plot of TBC-2 beam at 15.8 cm (6.2 in.) behind focal plane

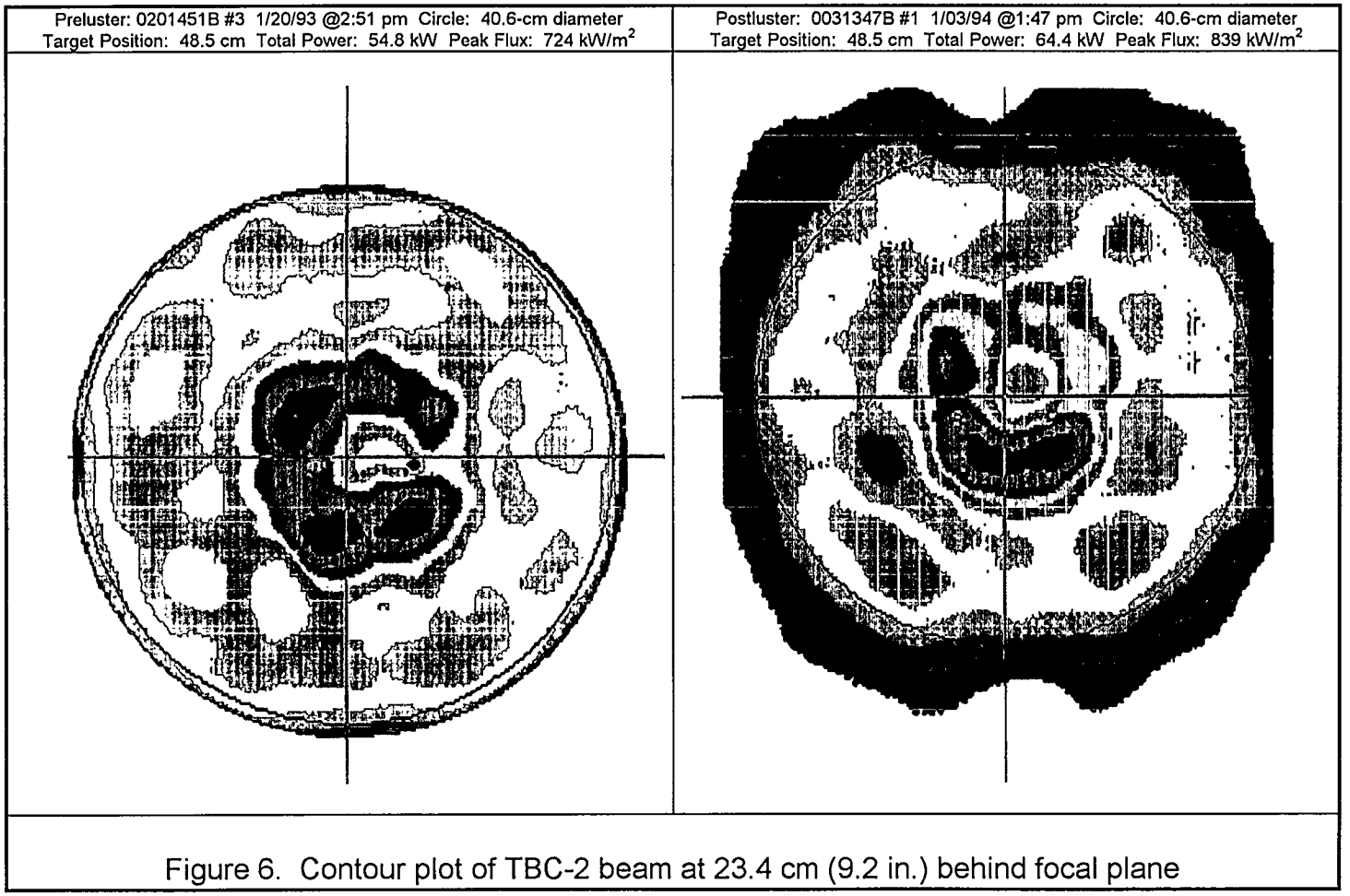

Figure 6. Contour plot of TBC-2 beam at 23.4 cm (9.2 in.) behind focal plane

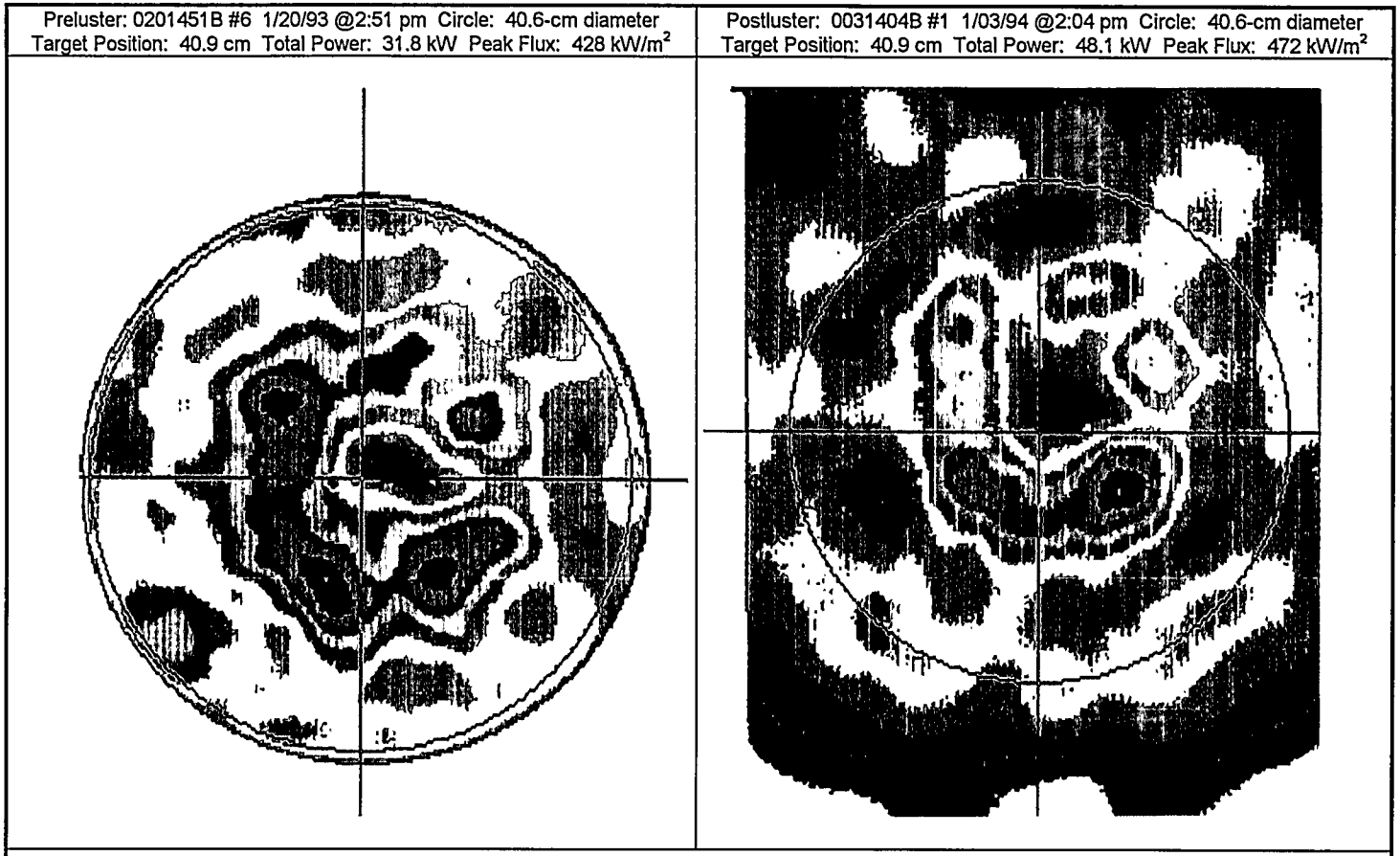

Figure 7. Contour plot of TBC-2 beam at 31.0 cm (12.2 in.) behind focal plane

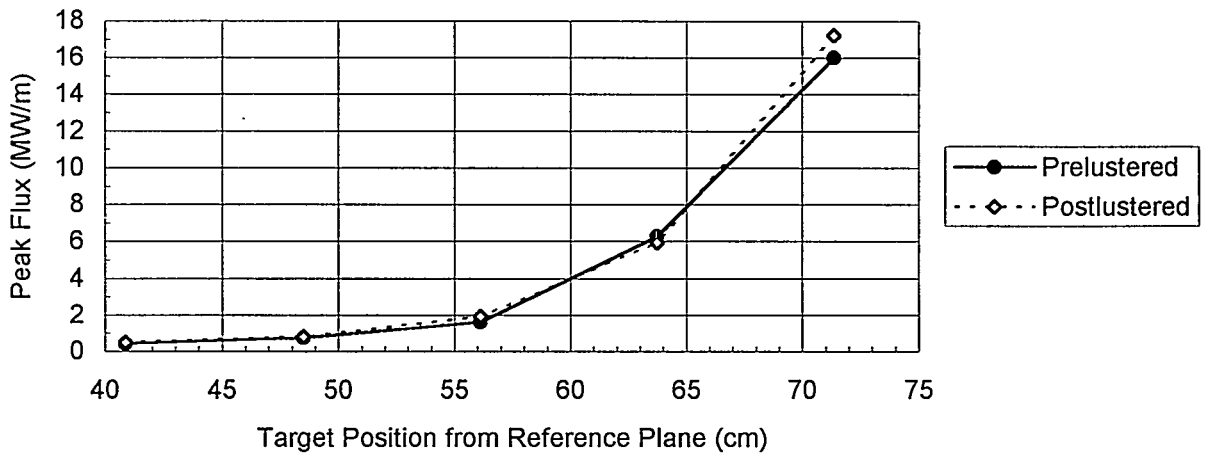

Figure 8. Peak flux measurements before and after lustering process

Table 2. Peak Flux and Total Power Measurements at the Focal Point

Distance from mounting plane (cm)	Distance from focal plane (cm)	Peak flux Normalized to Calorimetry Power (as indicated below) (kW/m^2)	% Change in Peak Flux after Lustering (%)	Total Power Measured with BCS (kW)	% Change in BCS Measured Power after Lustering (%)
Before Lustering (data file:R93020R)		(Calorimeter Pwr: 70.5 kW)			
71.4	-0.5	16598	⇓	68.0	⇓
63.8	-8.1	6442		68.5	
56.1	-15.8	1693	⇓	67.5	⇓
48.5	-23.4	751		54.8	
40.9	-31.0	474	⇓	31.8	⇓
After Lustering (data file:R94003A)		(Calorimeter Pwr: 77.9 kW)			
71.4	-0.5	17953	8.2	74.7	9.9
63.8	-8.1	6606	2.5	70.2	2.5
56.1	-15.8	2183	28.9	68.1	0.9
48.5	-23.4	900	19.9	62.1	13.3
40.9	-31.0	553	16.5	35.2	10.7

Beam Size

The beam size at TBC-2's focal point appears to be unchanged by the lustering and realignment processes. At its focus, which tests located at 71.8 cm (28.3 in.) from the reference plane, the measured beam diameter was 11.0 ±0.2 cm before and 10.8 ±0.2 cm after the reconditioning of the mirror facets. Beam diameter is defined as the diameter of a circle containing all flux in a beam whose intensity is ≥10% of that beam's peak flux intensity.

Figure 9 provides a graphical view of the preluster and postluster beam diameters measured at the five axial positions in the dish's focal region (see Table 3 for numerical values).

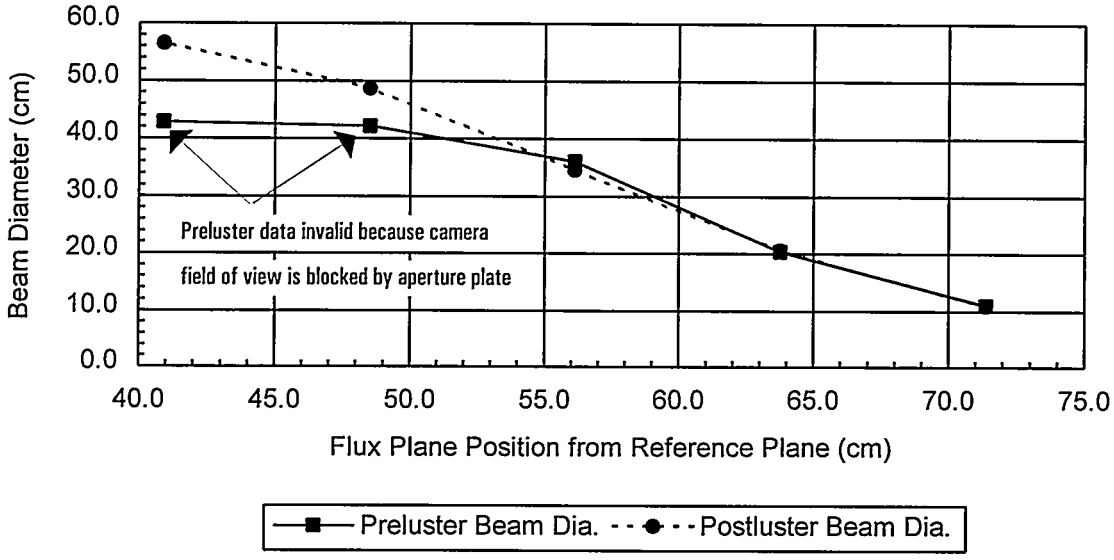

Figure 9. Beam diameter before and after lustering process

Table 3. TBC-2 Beam Diameter

BCS Target Position from Reference Plane (cm)	Preluster Beam Diameter (cm)—file: R093020R.WK1	Postluster Beam Diameter (cm)—file: R093020R.WK1
71.4	11.0	10.8
63.8	20.3	20.6
56.1	36.1	34.6
48.5	data invalid	48.7
40.9	data invalid	56.5

In the preluster test, the beam's diameter and power measurements were not accurate in the region 22.8 cm (9 in.) behind the focus (and beyond). An accurate measurement was prevented by the presence of the dish's aperture plate, which limited the BCS camera's field of view for the beam data obtained at the 22.8- and 30.4-cm (9- and 12-in.) positions behind the focus.[2] For the postluster test, the aperture plate was removed.

[2] During the preluster beam characterization the TBC-2 was equipped as usual with its aperture plate. This is a water-cooled flux shield that is typically mounted on the vertex side of the dish's mounting ring and provides a means of shielding the receiver or dish-test subject from the dish's intense beam of

Beam Power

Although excellent for characterizing collector flux distributions, the BCS is not particularly well-suited for making accurate beam power measurements. At Sandia, CWC is currently the preferred measurement, and calorimetry measurements of the TBC-2's total beam power were made in the same time frame as the preluster and postluster beam characterizations. The preluster and postluster calorimetry, performed in near-solar-noon conditions and subsequently normalized to an insolation level of 1,000 W/m^2, yielded total power values of 70.5 ± 1 and 77.9 ± 1 kW, respectively. Error analysis established the measurement accuracy at 1.5%. By contrast, the BCS accuracy is 6 to 10%. For this reason, the beam power measurements cited here are those made by calorimetry. For comparison purposes, Table 4 lists the TBC-2 power measurements made at or close to the focal plane obtained with both the BCS and the CWC.

Table 4. TBC-2 Power Measurements

	Preluster Beam Power	Postluster Beam Power
Beam Characterization (71.4 cm from reference plane)	68 ± 5 kW	75 ± 6 kW
Calorimetry (72.2 cm from reference plane)	70.5 ± 1 kW	77.9 ± 1 kW

Power Intercept

The lustering process increased the total dish power (from 70.5 ± 1to 77.9 ± 1 kW). Figure 10 provides power intercept curves that were obtained at two focal plane locations (71.4 and 63.8 cm (28.1 and 25.1 in.) from the dish reference plane) before and after the mirror reconditioning. Table 5 gives the data from which the curve was drawn. The power values were obtained from the BCS images or flux maps. The absolute accuracy of these beam power values is ± 8 to 10%, but the relative accuracy (i.e., the accuracy of one power value relative to the next) is ± 2 to 4%[3].

Beam Profile Analysis

The overall flux distribution in the TBC-2 beam does not appear to have been altered by the mirror lustering process. As another means of exploring this property, the beam profiles (a beam profile is essentially a cross section of the beam) of the TBC-2 before and after the lustering process were examined. Figure 11 compares the beam profiles at two focal plane locations

---

collected solar energy. The shield consists of a fixed, large circular aperture plate having a 40-cm (16-in.) diameter hole (through which the flux may pass), and a rectangular plate that can slide across the aperture to block the flux from reaching the receiver or whatever test apparatus is mounted in the focal region. During the postluster test this aperture plate was absent. Because the aperture plate is normally positioned between the BCS target and the BCS camera, the camera's view of the target is constrained by the 40-cm (16-in.) hole in the aperture plate. At a point around 17.7 or 20.4 cm (7 or 8 in.) behind the focal point, the dish's collected solar beam becomes wider than the 40-cm (16-in.) diameter, and that flux is not in the BCS camera's view. Thus, for the 22.8- and 30.4-cm (9- and 12-in.) positions behind the focal point, the preluster test was unable to measure flux outside the 40-cm (16-in.) inner circle of the flux target.

[3] The largest contributor to BCS measurement uncertainty is the calibration accuracy of the flux gauges. Relative power measurements (i.e., the power associated with individual picture elements in a BCS image) are obtained by image analysis without employing the flux gauges; their accuracy is unaffected by flux gauge inaccuracies.

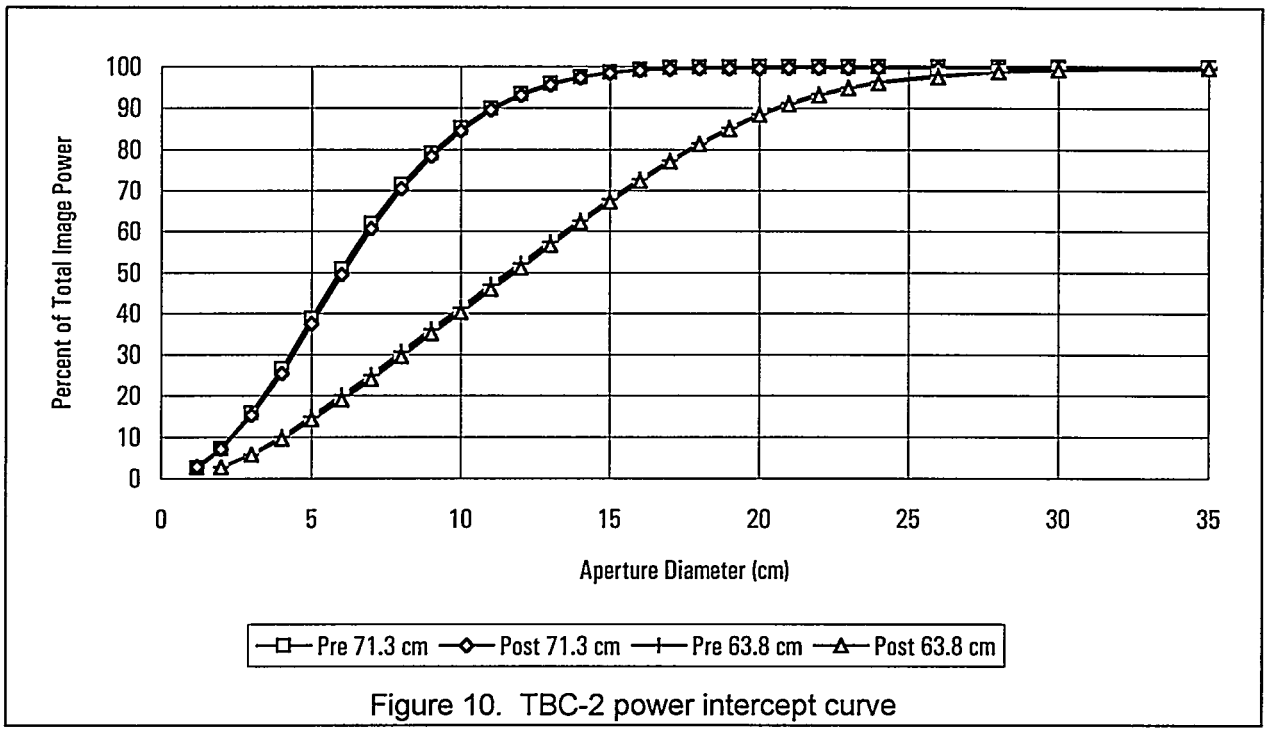

Figure 10. TBC-2 power intercept curve

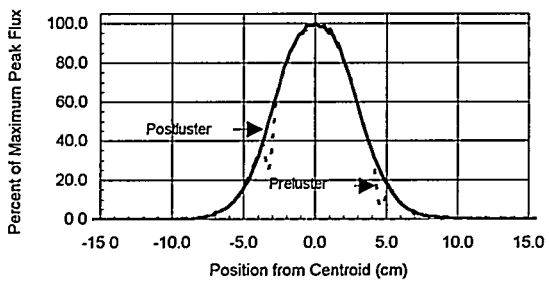

Horizontal Profile at 71.4 cm

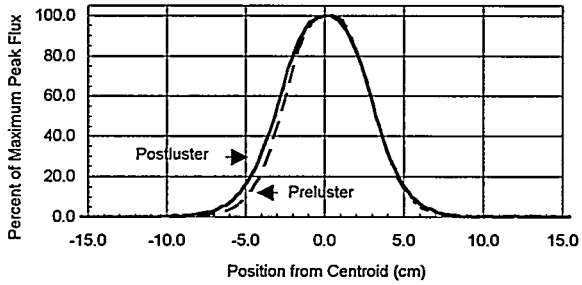

Vertical Profile at 71.4 cm

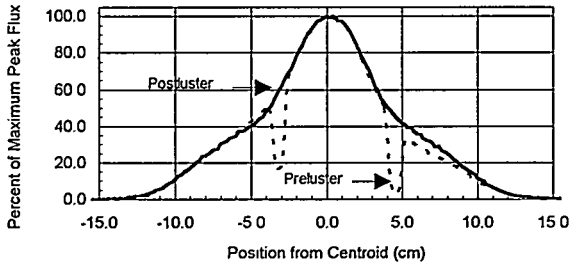

Horizontal Profile at 63.8 cm

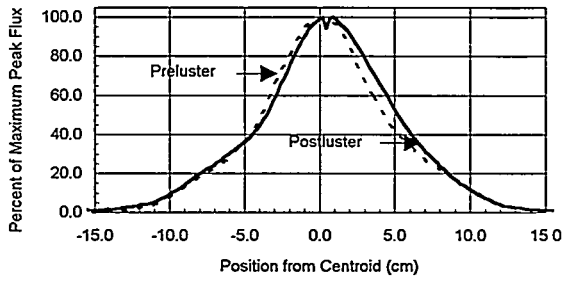

Vertical Profile at 63.8 cm

Figure 11. Profile plots of TBC-2 beams before and after lustering process

Table 5. BCS Image Power Data for Power Intercept Curve									
	Average Power (%)					Average Power (%)			
Aperture Diameter (cm)	71.4 cm from Reference Plane		63.8 cm from Reference Plane		Aperture Diameter (cm)	71.4 cm from Reference Plane		63.8 cm from Reference Plane	
	Before	After	Before	After		Before	After	Before	After
1.20	2.6	2.8			16.00	99.3	99.0	72.6	72.2
2.00	7.2	7.2	2.7	2.7	17.00	99.7	99.4	77.2	77.0
3.00	15.8	15.3	5.7	5.7	18.00	99.8	99.5	81.4	81.2
4.00	26.5	25.4	9.9	9.5	19.00	99.9	99.6	85.2	84.9
5.00	38.7	37.5	14.8	14.2	20.00	100.0	99.6	88.4	88.3
6.00	50.9	49.4	20.0	19.0	21.00	100.0	99.7	91.1	90.9
7.00	61.9	60.6	25.0	24.0	22.00	100.0	99.7	93.3	93.1
8.00	71.4	70.5	30.7	29.6	23.00	100.0	99.7	95.0	94.9
9.00	79.1	78.3	36.0	35.1	24.00	100.0	99.7	96.3	96.1
10.00	85.1	84.5	41.3	40.1	26.00	100.0	99.8	98.0	97.5
11.00	89.9	89.5	46.9	45.8	28.00	100.0	99.8	98.8	98.8
12.00	93.3	93.0	52.1	51.1	30.00	100.0	99.8	99.2	99.3
13.00	95.9	95.5	57.4	56.5	35.00	100.0	99.8	99.5	99.7
14.00	97.5	97.3	62.5	62.1	40.00	100.0	99.8	99.6	99.8
15.00	98.7	98.4	67.8	67.2					

before and after the mirror improvement process. No significant change in the TBC-2 beam is apparent.

CONCLUSION

The optical tests performed indicate that as a result of the mirror reconditioning and realignment process the location of the TBC-2's focal point did not change, but the dish's total power and peak flux capabilities did increase. The relative distribution of the flux in the collected beam appeared to remain qualitatively the same. The experimentally determined location of the dish's focal point remained at 71.8 cm (28.3 in.) toward the dish's vertex measured from the dish's receiver mounting plane. The normalized, overall power of the dish increased from 70.5 kW to 77.9 kW (± 1.1 kW), a change of 10.5%. The peak flux in the beam, measured at the focal point, increased from 16,598 kW/m^2 to 17,953 kW/m^2 (± 1,400 kW), a change of 8.2%. The diameter of the flux beam at the focal plane of the dish may have decreased slightly from 11.0 cm (± .2 cm) to 10.8 cm (± .2 cm). The relative flux distribution in the concentrated beam remained qualitatively unchanged.

REFERENCES

1. Strachan, J.W., 1992. *Testing and Evaluation of Large-Area Heliostats for Solar Thermal Application.* SAND92-1381. Sandia National Laboratories, Albuquerque, NM.

2. Strachan, J.W., 1993. "Revisiting the BCS, a Measurement System for Characterizing the Optics of Solar Collectors." SAND92-2789C. *Proceedings of the 39th International Symposium of the Instrument Society of America,* Albuquerque, NM.

UNLIMITED RELEASE
INITIAL DISTRUBUTION

3M Corporation
Construction Markets Department
R. Dahlen
3M Center Bldg. 207-1W-08
St. Paul, MN 55144-1000

3M Corporation
Solar Optics Program
P. Jaster
Bldg. 255-2N-06-3M Center
St. Paul, MN 55144-1000

Acurex Corporation
J. Schaeffer
555 Clyde Ave.
Mountain View, CA 94039

Advanced Thermal Systems
D. Gorman
7600 E. Arapahoe Rd., Ste. 215
Englewood, CO 80112

Alabama Solar Energy Center
L. Adcock
University of Alabama at Huntsville
Huntsville, AL 35899

Arizona Solar Energy Office
Department of Commerce
F. Mancini
3800 N. Central, Ste. 1200
Phoenix, AZ 85012

Arizona Public Service Company (2)
Thomas C. Lepley
P. Johnston
P.O. Box 53999
Phoenix, AZ 85072-3999

Arizona Public Service Company
Peter E. Eckert
1500 E. University
Tempe, AZ 85281

AT&T
Tom Maurer
P.O. Box 13369
Phoenix, AZ 85002

Battelle Pacific Northwest Laboratory
D. Brown
P.O. Box 999
Richland, WA 99352

California Energy Commission
Alec Jenkins
1516 Ninth St.
MS-43
Sacramento, CA 95814-5512

California Polytechnic State University (4)
William B. Stine
Department of Mechanical Engineering
3801 West Temple Ave.
Pomona, CA 91768-4062

Central and Southwest Services (2)
E. Gastineau
J. Schroeter
MS-7RES
1616 Woodall Rogers Freeway
Dallas, TX 75202

Clarkson University
E. Thatcher
Dept. of Mechanical and Aeronautical Engineering
Potsdam, NY 13699-5725

Clever Fellows Innovation Consortium, Inc.
J.A. Corey
R.D. 1, Box 410, River Rd.
Melrose, NY 12121

Cummins Power Generation
R. Kubo
Mail Code 60125
P.O. Box 3005
Columbus, IN 47202-3005

Cummins Power Generation South
Monte McGlaun
150 Tannehill Dr.
Abilene, TX 79602

Detroit Diesel Corporation (2)
P. Perdue
13400 Outer Drive West
Detroit, MI 48239-4001

Dynatherm Corporation
D. Wolf
1 Beaver Ct.
P.O. Box 398
Cockeyville, MD 21030

Electric Power Research Institute
J. Schaeffer
P.O. Box 10412
3412 Hillview Ave.
Palo Alto, CA 94303

Karl Thomas Feldman, Jr., Ph.D., P.E.
Mechanical Engineering Consultant
1704 Stanford Dr. NE
Albuquerque, NM 87106

Florida Solar Energy Center Library
300 State Rd., Ste. 401
Cape Canaveral, FL 32920-4099

Georgia Power Company
R. Kist
333 Piedmont Ave.
Atlanta, GA 30308

Hydrogen Engineering Associates (2)
H. Braun
4421 East Osborn
Phoenix, AZ 85018

Institute of Gas Technology
Library
34245 State St.
Chicago, IL 60616

Jet Propulsion Laboratory
M. Alper
4800 Oak Grove Dr.
Pasadena, CA 91109

Los Alamos National Laboratory
M. Merrigan
MS-E13
Los Alamos, NM 87545

McDonnell-Douglas Astronautics Company (3)
R.L. Gervais
J. Rogan
D. Steinmeyer
5301 Bolsa Ave.
Huntington Beach, CA 92647

Mechanical Technology, Inc. (2)
G. Dochat
J. Wagner
968 Albany Shaker Rd.
Latham, NY 12110

NASA/Lewis Research Center
R. Shaltens
21000 Brookpark Rd.
Cleveland, OH 44135

National Renewable Energy Laboratory (6)
M. Bohn
Gary Jorgensen
A. Lewandowski
L.M. Murphy
Tom Wendelin
Tom Williams
1617 Cole Blvd.
Golden, CO 80401-3393

Nevada Power Company
Eric Dominguez
P.O. Box 230
Las Vegas, NV 89151

New Mexico Solar Energy Institute
G. Mulholland
New Mexico State University
Box 3 SOL
Las Cruces, NM 88003

Northern Research & Engineering Corp.
James B. Kesseli
39 Olympia Ave.
Woburn, MA 01801-2073

Plains Electric Generation and Transmission
Cooperative, Inc.
D. Bailet
P.O. Box 6551
Albuquerque, NM 87197

Power Kinetics, Inc.
W.E. Rogers
415 River St.
Troy, NY 12180-2822

Research International
E. Saaski
18706 142nd Ave. NE
Woodinville, WA 98072

Rockwell International (2)
William Bigelow
R. LeChevalier
Energy Technology Engineering Ctr.
P.O. Box 1449
Canoga Park, CA 91304

Sacramento Municipal Utility District
Generation Systems Planning
Power Systems Department
Don Osborne
6201 'S' Street
Sacramento, CA 95852-1830

Salt River Project (2)
Research and Development
B. Hoffman
D. Osborn
P.O. Box 52025
Phoenix, AZ 85072-2025

SCAQMD (4)
R.S. George
J. Lents
A. Lloyd
L. Watkins
21865 Copley Dr.
Diamond Bar, CA 91765

Science Applications International Corp.
Kelly Beninga
10343 Roselle Street, Ste. G
San Diego, CA 92121

Science Applications International Corp.
B. Butler
Mail Stop 32
10260 Campus Point Ct.
San Diego, CA 92121

Solar Energy Industries Association
Ken Sheinkopf
777 N. Capitol St. NE, Ste. 805
Washington, DC 20002-4226

Solar Energy Industries Association
Scott Sklar
777 N. Capitol St. NE, Ste. 805
Washington, DC 20002-4226

Solar Kinetics, Inc. (2)
J.A. Hutchison
P. Schertz
P.O. Box 540636
Dallas, TX 75354-0636

Solar Reactor Technologies
Robin Parker
P.O. Box 330975
Miami, FL 33233

Southern California Edison Company (3)
Mark Skowronski
C. Lopez
J. Reeves
P.O. Box 800
Walnut Grove Ave.
Rosemead, CA 91770

Stirling Machine World
B. Ross
1823 Hummingbird Ct.
West Richland, WA 99352-9542

Stirling Technology Company (2)
M.A. White
2952 George Washington Way
Richland, WA 99352

Stirling Thermal Motors
L. Johansson
275 Metty Drive
Ann Arbor, MI 48103

Ken Stone
6882 Via Angelina
Huntington Beach, CA 92649

Sunpower, Inc. (2)
W. Beale
6 Byard St.
Athens, OH 45701

Tech Reps, Inc.
J. Stikar
5000 Marble NE, Ste. 222
Albuquerque, NM 87110

Thermacore, Inc. (2)
D. Ernst (4)
P. Dussinger
780 Eden Rd.
Lancaster, PA 17601

University of Chicago
J. O'Gallagher
Enrico Fermi Institute
5640 Ellis Ave.
Chicago, IL 60637

University of Houston
James Richardson
Solar Energy Laboratory
4800 Calhoun
Houston, TX 77704

University of Minnesota
E.A. Fletcher
111 Church St. SE
Department of Mechanical Engineering
Minneapolis, MN 55455

University of Nevada at Las Vegas
Mechanical Engineering Department
Bob Boehm
4505 Maryland Parkway
Las Vegas, NV 89154-4026

U.S. Department of Energy
R. Annan
Code EE-13
Forrestal Building
1000 Independence Ave. SW
Washington, DC 20585

U.S. Department of Energy (6)
Gary Burch (4)
Sig Gronich (2)
Code EE-132
Forrestal Building
1000 Independence Ave. SW
Washington, DC 20585

U.S. Department of Energy
Federal Energy Management Activities
Mark Ginsberg
EE-44
1000 Independence Ave., SW
Washington, DC 20585

U.S. Department of Energy
R. Hughey
San Francisco Operations Office
1333 Broadway
Oakland, CA 94612

U.S. Department of Energy
N. Lackey & G. Tennyson
Albuquerque Operations Office
P.O. Box 5400
Albuquerque, NM 87115

U.S. Department of Energy
Golden Field Office
Robert Martin
1617 Cole Blvd.
Golden, CO 80401

W.G. Associates
Vern Goldberg
6607 Stonebrook Cir.
Dallas, TX 75240

Energy Research Centre
K. Inall
R.S. Phy. Sc.
Autralian National University
Canberra ACT 2601, AUSTRALIA

David Hagen
134 Kitchener St.
Garran, ACT 2605, AUSTRALIA

DLR (2)
R. Buck
Reiner Köhne
Pfaffenwaldring 38 - 40
7000 Stuttgart 80 GERMANY

DLR - Cologne (3)
MD-ET
Linder-Höhne
M. Becker
M. Boehmer
P.O. Box 90 60 58
D-51140 Cologne GERMANY

Schlaich, Bergermann & Partner (2)
W. Schiel
Hohenzollernstr. 1
D-7000 Stuttgart 1, GERMANY

Internal Distribution:

MS0129	J. A. Leonard, 12611
0129	Lori Parrott, 12610
0444	N. J. Magnani, 5405
0703	C. E. Andraka, 6216 (2)
0703	R. B. Diver, 6216 (6)
0703	J. M. Chavez, 6215
0703	G. J. Kolb, 6216
0703	T. R. Mancini, 6216
0703	D. F. Menicucci, 6216
0703	J. E. Pacheco, 6216
0703	J.W. Grossman, 6216
0703	H. E. Reilly, 6216
0703	C. E. Tyner, 6216
0704	P. C. Klimas, 6201
0708	H. M. Dodd, 6214
0709	H. P. Stephens, 6212
0735	D. J. Alpert, 6200
0735	D. E. Arvizu, 6200
0749	A. P. Sylwester, 6203
0752	T. C. Bickel, 6213
0752	M. L. Whipple, 6219
0753	G. J. Jones, 6202
0753	C. P. Cameron, 6218
1127	Library, 6215 (3)
1127	R. M. Houser, 6215 (6)
0753	M. E. Ralph, 6218
1127	P. G. Cordeiro, 6215
1127	K. S. Rawlinson, 6215
1127	J. W. Strachan, 6215 (4)
9014	S. Faas, 5371
9015	A. Baker, 5908
0899	Technical Library, 13412 (5)
0619	Technical Publications, 12613
1119	Document Processing for DOE/OSTI, 7613-2 (2)
9018	Central Technical Files, 8523-2